Role of quantum nuclei and local fields in the x-ray absorption spectra of water and ice

Lingzhu Kong,[1] Xifan Wu,[2] and Roberto Car[3]

[1]*Department of Chemistry, Princeton University, Princeton, New Jersey 08544, USA*
[2]*Department of Physics, Temple University, Philadelphia, Pennsylvania 19122, USA*
[3]*Department of Chemistry and Department of Physics, Princeton University, Princeton, New Jersey 08544, USA*

We calculate the x-ray absorption spectra of liquid water at ambient conditions and of hexagonal ice close to melting, using a static GW approach that includes approximately local field effects. Quantum dynamics of the nuclei is taken into account by averaging the absorption cross section over molecular configurations generated by path integral simulations. We find that inclusion of quantum disorder is essential to bring the calculated spectra in close agreement with experiment. In particular, the intensity of the pre-edge feature, a spectral signature of broken and distorted hydrogen bonds, is accurately reproduced, in water and ice, only when quantum nuclei are considered. The effect of the local fields is less important but non negligible, particularly in ice.

PACS numbers: 61.25.Em, 61.05.cj, 71.15.Qe, 82.30.Rs

In the last decades high resolution core level spectroscopy, such as x-ray absorption spectroscopy (XAS) or x-ray Raman scattering (XRS), has emerged as a powerful tool for the investigation of matter at the molecular scale [1]. Important studies of liquid water and other disordered hydrogen-bond (H-bond) environments have been performed with these techniques [2–4]. Core spectroscopy is an element-specific local probe, complementary to diffraction for structural information, but requires a good theory of the excitation process as a prerequisite to a consistent experimental interpretation [5, 6]. Given that disordered environments need large cells and averages over different realizations, computationally efficient schemes based on density functional theory (DFT) have been the technique of choice in this context [7]. DFT, however, is not an excitation theory and yields spectra that are at best in semi-quantitative agreement with experiment.

Dramatic improvement in the calculated spectra is obtained with a proper excitation theory, as shown in a recent paper [8], which focused on water and adopted Hedin's GW approximation [9] for the self-energy of the excited electron in presence of a static core hole. Computationally, this approach is significantly more demanding than DFT and Ref. 8 compromised on the structural model and the screening approximation. The calculated spectrum deviated from experiment mostly in the pre-edge intensity which was underestimated by ∼50%. It was unclear if this discrepancy was due to limitations of the structural model, the screening model, or both. Ref. 8 used liquid structures generated by *ab initio* molecular dynamics (AIMD) [10] in a periodic cell with 32 H_2O molecules. With standard DFT approximations and classical nuclear dynamics this scheme yields enhanced water structure. Thus the temperature of the simulation was set to $T \sim 360K$ to improve agreement with experiment at ambient conditions ($T = 300K$). In addition, a simple uniform screening model was adopted, neglecting the microscopic inhomogeneity of the medium. The same paper reported also the spectrum of a proton ordered cubic ice structure that minimized the DFT energy at $T = 0K$. The deviation from experiment was significantly larger than in water, but one should recall that in real cubic (Ic) or hexagonal (Ih) ices, the distribution of the protons in the H-bonds is disordered. Moreover, the effect of zero-point motion was ignored. This is large, reflecting the quantum character of the nuclei, particularly the protons, signaled by neutron scattering experiments [11].

In this paper we address the above issues. We take the quantum character of the nuclei into account using molecular structures generated by path integral *ab initio* molecular dynamics (PI-AIMD) [12] for water at $T = 300K$ and for ice at $T = 269K$ [13]. In addition, we improve the treatment of screening by including, albeit approximately, the local fields due to the inhomogeneity of the medium within the Hybertsen-Louie (HL) ansatz [14]. We adopt larger simulation cells than in Ref. 8 and reduce the statistical error in the averages. Quantum effects bring the pre-edge intensity in close agreement with experiment in both water and ice. In addition, they reduce the post-edge intensity, for a better agreement with experiment, especially in water. Local field effects are modest in water, but cannot be neglected in ice that has a more open and less homogeneous microscopic structure. Here they improve the spectra in the main region that includes near- and post-edge, but some residual discrepancies remain, suggesting that a more accurate screening model could further improve the experimental comparison. Even at this stage, however, our approach, combining accurate *ab initio* simulations and spectral calculations, is a powerful interpretive tool for x-ray spectroscopy.

We base our calculations on the molecular structures of Ref. 13, which were obtained with PI-AIMD simulations using the BLYP functional [15, 20] for the electronic energy within DFT. The corresponding classical

AIMD structures with the same functional approximation and thermodynamic conditions were also reported in the same paper. Quantum nuclei soften the structure of water predicted by DFT, thereby greatly improving the experimental agreement of the calculated pair correlation functions. Residual overstructuring can be attributed to limitations of the functional approximation. Quantum dynamics increases the fraction of broken bonds and broadens the distribution functions. Thus, empirical adjustments like increasing the temperature of the simulation as in Ref. 8 can be avoided. Ref. 13 used open PI trajectories [16] to calculate the momentum distribution of the protons, finding excellent agreement with deep inelastic neutron scattering experiments. Relative to its classical counterpart, the quantum momentum distribution is strongly displaced towards higher momenta and deviates significantly from a spherical Gaussian distribution [17], indicating that a higher effective temperature in classical simulations can only be a poor surrogate of full quantum simulations. The latter are based on Feynman paths in imaginary time, which provide an exact representation of equilibrium quantum statistical mechanics. The x-ray absorption cross section is a dynamic property requiring, in principle, path components in real time which would carry a complex phase not amenable to computer simulation, but we can rely on the wide separation of time scales between nuclear and electron dynamics, in the spirit of the Franck-Condon principle. In the present case it amounts to compute the spectra for the frozen nuclear configurations sampled with the adopted discrete representation of the Feynman paths in imaginary time.

Molecular configurations for water at $T = 300K$ and ice Ih at $T = 269K$ were generated in Ref. 13 by adopting the "bulk" approximation in which the Feynman path of one proton per molecule is left open to improve the statistics of the momentum distribution [13, 16]. It was shown that this approximation has negligible effect on the momentum distribution and very minor effect on the spatial correlations between the protons [16]. The simulations used a periodic cell with 64 molecules for water and 96 molecules for ice Ih in a proton disordered configuration with cell volumes fixed to experiment. The Feynman paths were discretized using 32 replicas in both cases. In our XAS calculation we use the static Coulomb hole and screened exchange (COHSEX) approach of Ref. [8] and average the excitation cross section over all the molecules in the cell. We include quantum effects by averaging over path-integral replicas. Each particle (H or O nucleus) path runs in imaginary time from $\tau = 0$ to $\tau = \hbar/k_BT$. To minimize the effect of the open paths we only include in the average 26 middle path replicas in water and 16 in ice as this was sufficient for convergence. Even limiting the average to a fraction of the replicas, the number of calculations is huge and we consider only a single molecular dynamics snapshot to reduce the computational burden.. We checked for classical nuclei that this has minor effect on the spectra. Aiming at further reducing the computational cost, we have investigated whether calculations at the centroids of the paths could capture most quantum effects. Unfortunately, this was not the case. In water, centroid calculations led to a pre-edge intensity approximately half-way between classical and quantum data, consistent with the observation that the fraction of broken bonds is approximately the same in the centroid and path structures. In ice, that has no broken bonds, the centroid spectrum was indistinguishable from the classical one.

We include local fields in the screening by means of the HL local density approximation according to which the screened interaction reads [14]

$$W(\mathbf{r},\mathbf{r}') = \frac{1}{2}\left(W[\mathbf{r}-\mathbf{r}';\rho(\mathbf{r}')] + W[\mathbf{r}'-\mathbf{r};\rho(\mathbf{r})]\right) \quad (1)$$

Eq.(1) is based on the observation that the screening strength generally follows the local charge density. Here

$$W[\mathbf{r}'-\mathbf{r};\rho(\mathbf{r})] = \frac{1}{(2\pi)^3}\int \epsilon^{-1}[\mathbf{q};\rho(\mathbf{r})]v(\mathbf{q})e^{i\mathbf{q}\cdot(\mathbf{r}-\mathbf{r}')}\,d\mathbf{q} \quad (2)$$

and v is the bare Coulomb interaction. For the dielectric function, we adopt Bechstedt model [18],

$$\epsilon[\mathbf{q},\rho(\mathbf{r})] = 1 + [(\epsilon_0-1)^{-1} + \alpha(\frac{q}{q_{TF}})^2 + \frac{q^4}{4\omega_p^2}]^{-1} \quad (3)$$

where q_{TF} and ω_p denote Thomas-Fermi wavevector and plasmon frequency, respectively. These quantities depend on the local density but in Ref. [8] dependence on the average density was assumed. The $q = 0$ value ϵ_0 is taken from experiment and α is fixed by requiring Bechstedt model (Eq.(3)) to match the q^2 dependence of Penn model [19]. Eq. (2) can be analytically evaluated yielding

$$W[\mathbf{r}'-\mathbf{r};\rho(\mathbf{r})] = \frac{v(\mathbf{r}-\mathbf{r}')}{\epsilon_0} - \frac{1}{a(x_1-x_2)|\mathbf{r}'-\mathbf{r}|}\left(\frac{e^{i(x_1)^{1/2}|\mathbf{r}'-\mathbf{r}|}}{x_1} - \frac{e^{i(x_2)^{1/2}|\mathbf{r}'-\mathbf{r}|}}{x_2}\right) \quad (4)$$

where $x_{1,2} = (-b \pm \sqrt{b^2-4ac})/2a$ and $a = 1/4\omega_p^2$, $b = \alpha/q_{TF}^2$ and $c = \epsilon_0/(\epsilon_0-1)$. There are two con-

tributions to the screened interaction W in Eq. (4), the bare interaction v divided by the macroscopic dielectric constant, and a local-density dependent screened interaction, which is fully nonlocal but short-ranged in space. To evaluate the effect of W on the self-energy we use the convolution theorem for the part depending on the bare interaction, which is conveniently calculated in Fourier space, and we compute the integral in real space for the short-ranged nonlocal contribution.

Fig. 1 shows the calculated XAS intensity for liquid water and ice Ih at different levels of approximation. The spectra are aligned at the onset and the absorption sum rule is imposed to fix the normalization so that the spectra have equal area in the energy range of the figure. Hartree-Fock results are also reported: they correspond to calculations with the dielectric function set equal to 1, i.e. ignoring screening.

Replacing classical with quantum nuclei affects the spectra, because zero-point motion significantly enhances the positional disorder relative to classical thermal motion. Qualitatively similar conclusions were reached in a recent study of the XAS spectrum of ice using PI configurations generated with an empirical intermolecular potential [20]. In addition, quantum fluctuations increase the fraction of broken H-bonds in the liquid by ∼4% [13]. As a consequence pre-edge is increased, post-edge is reduced and there is an overall slight broadening of the spectrum. The effects on pre- and post-edge are more pronounced in the liquid, where the post-edge is particularly interesting as it correlates with the less overstructured H-bond network of the quantum simulations.

Local fields have comparatively smaller effects than quantum nuclei. Here it is useful to start from Hartree-Fock. In this limit screening is absent, the quasi-particle excitation energies are overestimated resulting in too wide spectra with the post-edge more prominent than the near-edge in both water and ice. COHSEX calculations improve the agreement with experiment, by reducing the overall width and by lowering post-edge below near-edge in the liquid. The difference between the spectra with a uniform screening model and those obtained with the HL local density approximation is a measure of the inhomogeneity of matter at the molecular scale, which renders screening less effective than in the corresponding uniform medium. Local fields are underestimated in the HL approach [9] and one should expect that screening would be further reduced in a more accurate theory. The effect should be small in water where the HL induced change is minor, but in ice the HL induced change is non negligible suggesting that a better screening model should move the spectrum further in the Hartree-Fock direction..

In Fig. 2 our results with quantum nuclei and COHSEX with local fields, are compared to XAS and XRS experiments. The spectra are aligned at the onset and normalized by the same area. The difference spectrum in the bottom panel of the figure is obtained by subtracting ice from water intensity dividing the result by the integrated spectral area. The accord among experiments is excellent: the only noticeable difference between XAS and XRS in the post-edge of ice may reflect differences in the experiments and the samples. Overall the agreement between theory and experiment is quantitatively good in both water and ice. In the latter case, the dramatic improvement relative to Ref. [8] is a strong indication of the importance of a realistic model of disorder not only in liquid but also in crystalline water. The agreement between theory and experiments in the pre-edge is particularly satisfying given that most previous calculations failed to reproduce the correct relative intensity of this feature, associated to a bound exciton mostly localized on the excited molecule [8, 22]. Based on the quantum-classical trends in Fig. 1 we should expect that isotope effects should be detectable: making the protons more classical should weaken the pre-edge and strengthen the post-edge. Remarkably, this has been observed in high resolution XAS measurements on liquid H_2O and D_2O samples [23]. The main remaining difference between theory and experiment in the water spectrum is a small overestimate of the post-edge intensity.

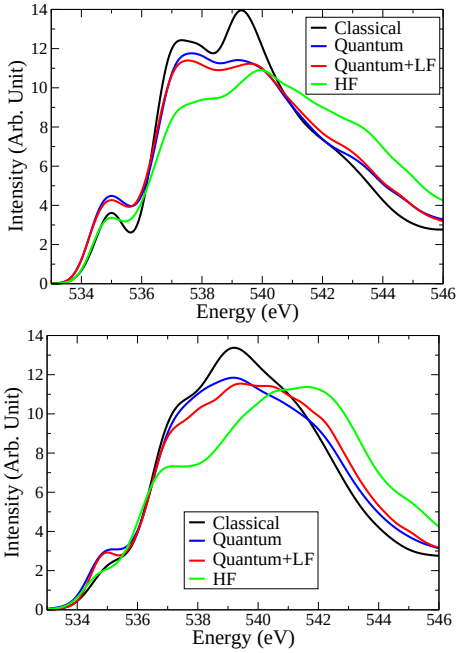

FIG. 1: (Color online) Calculated XAS spectra for liquid water at $T = 300K$ (top) and ice Ih at $T = 269K$ (bottom) according to four different schemes: (a) COHSEX with classical nuclei and uniform screening (black); (b) COHSEX with quantum nuclei and uniform screening (blue); (c) COHSEX with quantum nuclei and local field (LF) screening (see text) (red); (d) Hartree-Fock with quantum nuclei (green). The spectra are area normalized and Gaussian broadened(fwhm=0.4 eV). In order of increasing energy, three features, the pre-edge, the near-edge, and the post-edge, characterize the spectra.

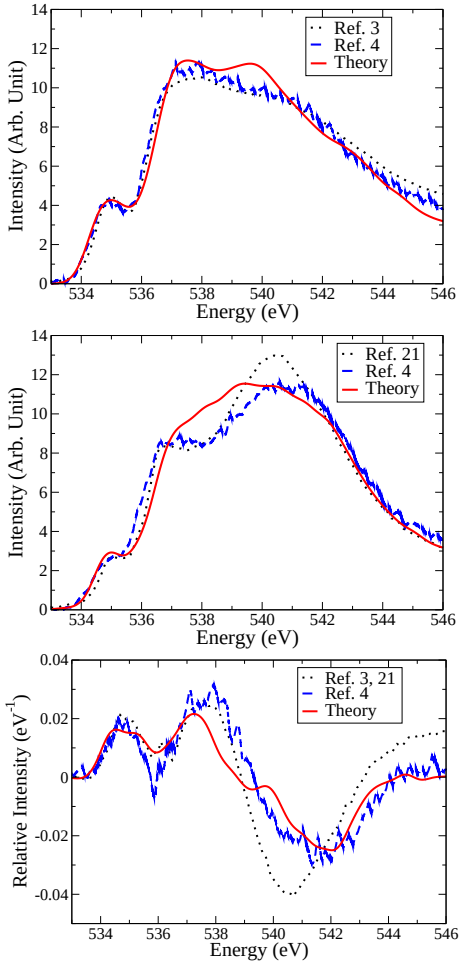

FIG. 2: (Color online) Comparison of calculated XAS spectra with experiments for water (top), ice Ih (middle) and the difference between water and ice Ih (bottom). Two sets of experimental data are included for each system [3, 4, 21]. Water is at room temperature in theory and experiments, ice is at $T = 269K$ in the present calculation, at $T = 130K$ in [21] and at $T = 40K$ in [4]. The difference spectrum is obtained from [I(water)-I(Ih)]/S where I denotes spectral intensity and S is the integrated area of the spectra in the energy range of the figure.

This may reflect residual overstructuring present in the H-bond network of the PI-AIMD simulations, a conclusion also borne by the analysis of the radial distribution functions [13]. We think that this inaccuracy is due to limitations of the BLYP functional approximation. Improved approximations including hybrid exchange that reduces the self-interaction error [24] and including dispersion (van der Waals) interactions would further soften the network structure [25] weakening the post-edge feature. The difference between ice and water in the relative strength of near- and post-edge features has its origin in the partial collapse of the H-bond network that brings a non-bonded molecular fraction within range of the first coordination shell in the liquid [8]. The corresponding "interstitial" molecules do not form H-bonds with the central molecule but are H-bonded to molecules outside the coordination shell. This interpretation is consistent with diffraction studies [26] and we confirm it here. Quantum nuclei are crucial in water because they enhance the network collapse compared to classical simulations. This effect is absent in ice Ih, which has an intact tetrahedral network with coordination 4 [27]. In ice the residual differences between theory and experiments in the main edge may reflect to some extent the different temperatures of the simulation and the experiments. However, thermal effects should be small as the vibrational spectrum is largely ground-state dominated [17]. We think that the differences should mostly reflect the adopted screening approximation, which underestimates local fields. A more accurate screening model should enhance post-edge at the expense of near-edge, improving the agreement with experiment. A fully first-principles treatment of static screening would be possible but computationally very demanding. Finally, we have neglected the energy dependence of the self energy, which should affect the calculated spectra, particularly at high energy. Such effects could be included either via a dynamic COHSEX calculation or, simply, with phenomenological schemes such as rescaling the energy axis or using an energy-dependent broadening function [28, 29]. The good agreement between experiment and theory found in the present study suggests that these effects should be small in water and ice.

In conclusion, we have improved an approach to calculate the XAS spectra of disordered environments [8], by including local field effects beyond the uniform screening approximation. The most important result of the present investigation has been, however, to elucidate the role of nuclear quantum dynamics on the spectra of water and ice. On one hand zero point motion broadens the spectra via Franck-Condon factors that we calculate by averaging over the distribution of the Feynman paths. On the other hand quantum nuclei modify the liquid structure by facilitating H-bond breaking. Our analysis shows that many competing factors are important to reproduce the spectral differences observed between water and ice. In view of its ability to probe local environments, x-ray spectroscopy is a very important tool for investigating not only bulk neat water, as done here, but also water solutions, water at interfaces, and, in general, soft condensed matter environments like bio-molecular solutions. The theoretical techniques developed here should contribute to these studies by giving insight on the origin of the spectral features and by allowing us to connect these features to the details of the local molecular structure.

The authors thank J. A. Morrone for providing the path integral structures and acknowledge fruitful and stimulating discussions with L.G.M. Pettersson and A. Nilsson. This work was supported by the NSF under grant CHE-0956500 and by the U.S. Department

of Energy under grants de-sc0005180 and DE-FG02-05ER4201. The calculations were performed at the National Energy Research Scientific Computing Center, which is supported by the Department of Energy under Contract DE-AC02-05CH11231.

[1] J. Stohr, Nexafs Spectroscopy (Springer-Verlag, New York, 1992).
[2] K. R. Wilson, B. S. Rude, T. Catalano, R. D. Schaller, J. G. Tobin, D. T. Co, and R. J. Saykally, J. Phys. Chem. B **105**, 3346 (2001).
[3] P. Wernet, D. Nordlund, U. Bergmann, M. Cavalleri, M. Odelius, H. Ogasawara, L. A. Näslund, T. K. Hirsch, L. Ojamäe, P. Glatzel, et al., Science **304**, 995 (2004).
[4] J. S. Tse, D. M. Shaw, D. D. Klug, S. Patchkovskii, G. Vankó, G. Monaco, and M. Krisch, Phys. Rev. Lett. **100**, 095502 (2008).
[5] J. Vinson, J. J. Rehr, J. J. Kas, and E. L. Shirley, Phys. Rev. B **83**, 115106 (2011).
[6] J. Vinson, J. J. Kas, F. D. Vila, J. J. Rehr, and E. L. Shirley, Phys. Rev. B **85**, 045101 (2012).
[7] B. Hetényi, F. D. Angelis, P. Giannozzi, and R. Car, J. Chem. Phys. 120, 8632 (2004); M. Cavalleri, M. Odelius, A. Nilsson, and L. G. M. Pettersson, J. Chem. Phys. 121, 10065 (2004). D. Prendergast and G. Galli, Phys. Rev. Lett. 96, 215502 (2006);.
[8] W. Chen, X. Wu, and R. Car, Phys. Rev. Lett. **105**, 017802 (2010).
[9] G. Onida, L. Reining, and A. Rubio, Rev. Mod. Phys. **74**, 601 (2002).
[10] R. Car and M. Parrinello, Phys. Rev. Lett. **55**, 2471 (1985).
[11] S. Bratos, M. Diraison, G. Tarjus, and J-Cl. Leicknam, Phys Rev A 45, 5556 (1992); C. Andreani, D. Colognesi, J. Mayers, G.F. Reiter, and R. Senesi, Adv. Phys. 54, 377 (2005).
[12] D. Marx and M. Parrinello, Z. Phys. B Cond. Mat. **95**, 143 (1994).
[13] J. A. Morrone and R. Car, Phys. Rev. Lett. **101**, 017801 (2008).
[14] M. S. Hybertsen and S. G. Louie, Phys. Rev. B **37**, 2733 (1988).
[15] A. D. Becke, Phys. Rev. A **38**, 3098 (1988).
[16] J. A. Morrone, V. Srinivasan, D. Sebastiani, and R. Car, J. Chem. Phys. **126** (2007).
[17] L. Lin, J. A. Morrone, R. Car, and M. Parrinello, Phys. Rev. B **83**, 220302 (2011).
[18] F. Bechstedt, R. D. Sole, G. Cappellini, and L. Reining, Solid State Commun. **84**, 765 (1992).
[19] D. R. Penn, Phys. Rev. **128**, 2093 (1962).
[20] C. Lee, W. Yang, and R. G. Parr, Phys. Rev. B **37**, 785 (1988).
[21] A. Nilsson, H. Ogasawara, M. Cavalleri, D. Nordlund, M. Nyberg, P. Wernet, and L. G. M. Pettersson, J. Chem. Phys. **122**, 154505 (2005).
[22] D. Nordlund, H. Ogasawara, H. Bluhm, O. Takahashi, M. Odelius, M. Nagasono, L. G. M. Pettersson, and A. Nilsson, Phys. Rev. Lett. **99**, 217406 (2007).
[23] U. Bergmann, D. Nordlund, P. Wernet, M. Odelius, L. G. M. Pettersson, and A. Nilsson, Phys. Rev. B **76**, 024202 (2007).
[24] A. J. Cohen, P. Mori-Snchez, and W. Yang, Science **321**, 792 (2008).
[25] Z. Li, X. Wu, R. DiStasio Jr. and R. Car, http://meetings.aps.org/Meeting/MAR12/Event/161365.
[26] J. L. Finney, A. Hallbrucker, I. Kohl, A. K. Soper, and D. T. Bowron, Phys. Rev. Lett. **88**, 225503 (2002).
[27] Structures in which tetrahedrally bonded molecules penetrate the first coordination shell without forming a bond with the central molecule are found in high-pressure ice phases, an extreme case being that of ice VIII and VII.
[28] G. Materlik, J. E. Müller, and J. W. Wilkins, Phys. Rev. Lett. **50**, 267 (1983).
[29] J. Rehr, Radiat. Phys. Chem. **75**, 1547 (2006).